Heliyon 8 (2022) e11415

Contents lists available at ScienceDirect

Heliyon

journal homepage: www.cell.com/heliyon

Research article

Shape programmable magnetic pixel soft robot

Ran Zhao [a,b,c], Houde Dai [a,c,*], Hanchen Yao [a,c], Yafeng Shi [b], Guopeng Zhou [a,d]

[a] Quanzhou Institute of Equipment Manufacturing of Haixi Institutes, Chinese Academy of Sciences, Quanzhou 362200, China
[b] Zhongyuan-Petersburg Aviation College, Zhongyuan University of Technology, Zhengzhou 450000, China
[c] Fujian Institute of Research on the Structure of Matter, Chinese Academy of Sciences, Fuzhou 350000, China
[d] School of Electrical and Control Engineering, North University of China, Taiyuan 030000, China

GRAPHICAL ABSTRACT

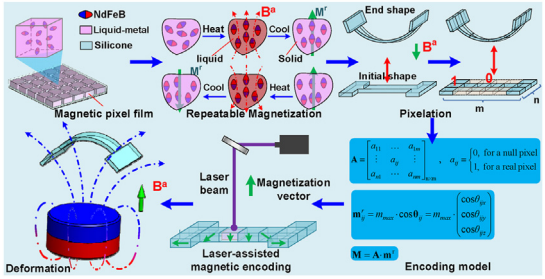

Principle of magnetic pixel soft robot.

ARTICLE INFO

Keywords:
Soft robot
Magnetic pixel
Magnetic encoding
Programmable shape
Liquid-metal

ABSTRACT

Magnetic soft robots (MSRs) can achieve controllable shape-morphing by magnetic programming to the magnetic elastomer. However, the magnetization profile is usually implemented on a continuous region and is unchangeable. The deformation and function design of MSR hence is limited. This study presents a programmable magnetic pixel soft robot (MPSR). By encapsulating liquid-metal/NdFeB composites into a Silicone shell, the thermal-magnetic response functional film with lattice-structure is fabricated, with the highest pixel resolution of 1×1 mm^2. A piece of laser-assisted magnetic programming equipment is developed to implement magnetic encoding on discrete regions of the film. Therefore, a mathematical model is proposed to help calculate the magnetic codes according to the preset end shape. At last, several pixel-structure MPSRs are prepared and tested. Experimental results show that using the magnetic encoding technique, we can reconfigure the deformations and functions of the robot. This study provides a basis for the programmed shape regulation and motion design of the soft robot.

1. Introduction

Magneto-actuated soft robots, as a kind of untethered robot, can implement multiple tasks such as cell manipulation, medical image acquisition, drug delivery, and noninvasive intervention. Compared to light/thermal, chemical, or electrical actuated soft robots [1, 2, 3, 4], magnetic soft robots have the advantages of fast response, unlimited endurance, no obstruction restrictions, and magnetically traceable [5, 6, 7, 8]. Therefore, significant progress has been achieved in recent years.

The motion of a magnetic soft robot comes from the response of magnetic particles wrapped in a flexible matrix when applying a magnetic field. These particles can be soft magnetic materials, such as Fe, Ni, and Fe_3O_4 [9,10], or hard magnetic materials, e.g., CrO_2 and $Nd_2Fe_{14}B$ [11, 12, 13]. The soft robot based on hard magnetic materials has high

* Corresponding author.
E-mail address: dhd@fjirsm.ac.cn (H. Dai).

https://doi.org/10.1016/j.heliyon.2022.e11415
Received 27 May 2022; Received in revised form 12 July 2022; Accepted 1 November 2022

residual magnetization. The shape morphing is performed by configuring the magnetic anisotropy, i.e., magnetic programming or magnetic encoding. By far, there are still some technical limitations in MSR. For one thing, MSR's magnetizing process is coupled with its manufacturing process. This leads to the irreversibility of the magnetization profile and single function of MSR. Therefore, shape memory polymers are introduced to manufacture reprogrammable magnetic elastomer [14, 15]. By heating to the elastomer, magnetic particles are reoriented and then locked when the matrix media is in the solid phase. But the heating temperature is too high (>60 °C) for biomedical applications. For another, the magnetic programming technique is usually implemented in continuous media [16, 17, 18]. There is no obvious boundary between differently magnetized regions, which is disadvantageous to the computable and refine magnetization profile design. To this end, Cui *et al.* proposed the concept of magnetic encoding, i.e., a technique to generate a magnetic response by coding magnetization vectors on discrete programmable units [19]. But this technique can only deal with vertical vector coding and lacks sufficient flexibility in deformation design.

In short, it is a great challenge to develop a technique that can simultaneously realize repeatable, low-temperature and arbitrary vector directional magnetic encoding. The previous work introduced a technique of reprogrammable magnetization based on Liquid-metal/NdFeB/Silicone composites [20]. The developed liquid-metal MSR can accomplish reprogrammable deformation. On this basis, a robot based on the lattice-structure magneto-elastomer, named magnetic pixel soft robot, is presented. A 3D vector magnetization equipment was developed to perform magnetic encoding to the composite film. In addition, a standard magnetic encoding procedure is exhibited for the calculation-based deformation planning. Several cases demonstrate how the MPSR performs shape-morphing planning and changes the responses through magnetic encoding. The details are given in the following sections.

2. Methodology

2.1. Magnetic vector programming system

Figure 1a shows the physical apparatus for patterning three-dimensional (3D) discrete magnetization in Liquid-metal/NdFeB/Silicone composite films. The apparatus consists of a triple-axis positioning platform, a 2-DOF rotation platform, a triple-axis Hall sensor, a square magnet (N52, 24 × 24 × 24 mm^2, surface magnetic intensity of 435 mT), a semiconductor cooler, and a coaxial optical system including a 405 nm ultraviolet laser and a charge-coupled-device (CCD) camera. A 3D vector magnetic field of any direction and strength can be generated based on the 5-axis motion platform. In addition, the magnetic vector is measured by a 3D Hall sensor (MS2GO, Infineon Inc., Germany). A 20 mW ultraviolet (UV) laser with 800 μm resolution is employed to heat the magnetic pixel film (MPF). The semiconductor cooler is utilized to reduce the temperature of the non-heated region of the film. Finally, the functional film variation can be observed by the CCD camera.

2.2. Operation mechanism of the magnetic pixel soft robot

The proposed thermo-magnetic response functional film is made of Liquid-metal/NdFeB composites and then coated with silicone. As shown in Figure 1b, the film has a discrete lattice structure, where each primary cell is defined as a magnetic pixel. In each magnetic pixel, the NdFeB micro-particles are wrapped and uniformly distributed in the liquid-metal matrix.

Figure 1c exhibits the cycle process of the magnetic programming. When heating by a laser, gallium can be transformed from solid to liquid phase. NdFeB particles hence will be reoriented under the programming magnetic field, and form macro magnetic anisotropy, i.e., remanent magnetization (shown as the green arrow), in the heated region. The required heating temperature is 40 °C. After the magnetization process, the liquid metal is cooled, thereby converting it into solid phase. This process can be implemented repeatedly, which means multiple shape-morphing responses can be generated by encoding different magnetization profile schemes on the magnetic pixel film.

Figure 1d shows how to encode a magnetic pixel robot. The discrete regions of each pixel are heated by a low-energy laser separately, and then programmed with different magnetization vectors. Finally, a discrete magnetization profile can be obtained and the robot generates a specific shape deformation when applying an external magnetic field (Figure 1e).

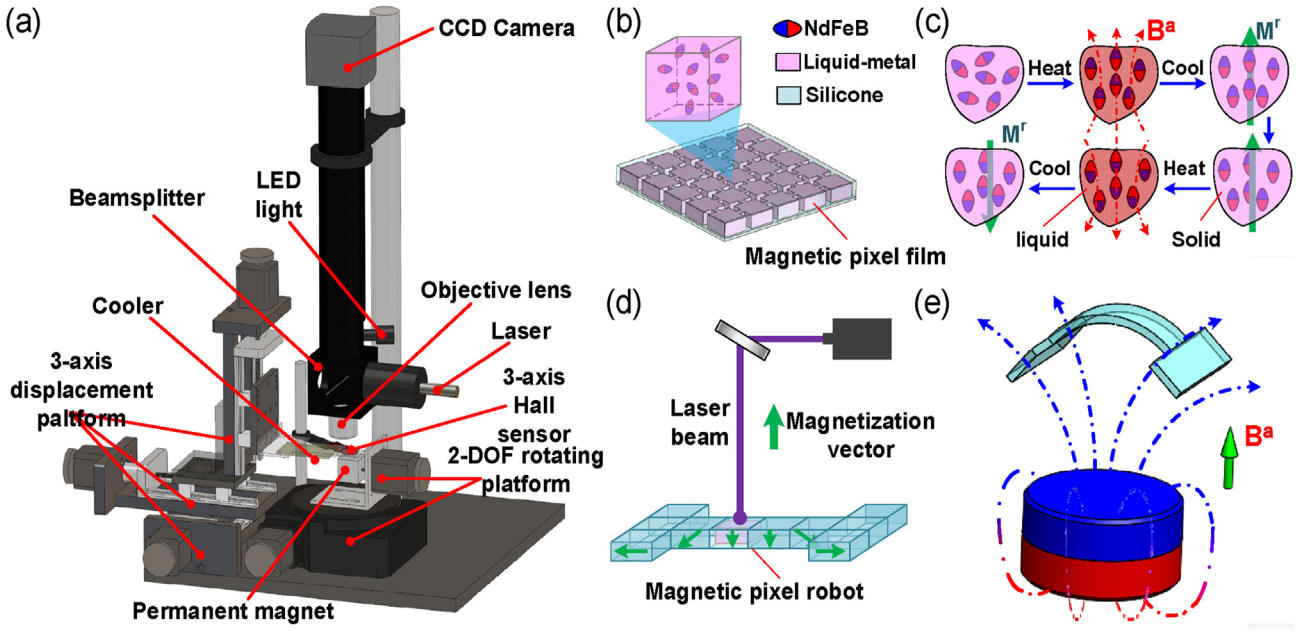

Figure 1. Principle of shape programmable magnetic pixel robot: (a) 3D magnetic vector programming system, (b) Structure of magnetic pixel film, (c) Mechanism of the Liquid-metal/NdFeB composites, (d) Magnetic encoding to the pixel robot, and (e) Magnetic response action.

3. Magnetic encoding technique

3.1. Encoding procedure

It is a great challenge to manufacture shape programmable magnetic soft robots in batch and automatically, due to the lack of the encoding method and model. At present, the planning of a robot's magnetization profile is often based on experience. Therefore, we presented a standard procedure and a mathematical description for 3D magnetic vector encoding. As shown in Figure 2, the encoding procedure includes the following two steps:

i. Pixelation process. As shown in Figure 2a, the soft robot's initial shape (without the external magnetic field) and end shape (with the maximum external magnetic field) are designed. We can design more than one type of end shape to achieve multiple programmable deformations for MSR. This customized continuous shape is then meshed and decomposed into discrete pixels (Figure 2b). The mesh size determines the pixel lattices' resolution and the robot deformation's smoothness. We can transform any 2D plane shape into a MPSR through pixelation process.
ii. Encode planning. Figure 2c shows the scheme of the encode planning process. First, the magnetic vector angles are calculated according to the initial and end coordinates of each pixel (Figure 2d). Then these magnetic vectors are composed of a magnetic encoding matrix to program the robot.

3.2. Mathematical model

As exhibited in Figure 2b, a matrix **A** is employed to represent the pixel robot, as given in Eq. (1),

$$\mathbf{A}=\begin{bmatrix} a_{11} & \cdots & a_{1m} \\ \vdots & a_{ij} & \vdots \\ a_{n1} & \cdots & a_{nm} \end{bmatrix}_{n\times m}, a_{ij}=\begin{cases} 0 & \text{for a null pixel} \\ 1 & \text{for a real pixel} \end{cases} \tag{1}$$

where **A** is the geometry matrix, which describes the robot's geometry and loads the magnetic vector for coding.

The theoretical maximum magnetization m_{max} can be acquired after the dimensions of a pixel are determined. It is reasonable to utilize m_{max} as the modulus of the magnetic encoding vector, which can maintain the consistency of all magnetic pixels and make full use of the driving magnetic field. The *ij*-th magnetic encoding vector $\mathbf{m}^r_{ij}$ hence can be expressed as Eq. (2),

$$\mathbf{m}^r_{ij}=m_{max}\cdot\cos\boldsymbol{\theta}_{ij}=m_{max}\cdot\begin{pmatrix}\cos\theta_{ijx}\\ \cos\theta_{ijy}\\ \cos\theta_{ijz}\end{pmatrix}, \tag{2}$$

where $\boldsymbol{\theta}_{ij}=(\theta_x,\theta_y,\theta_z)_{ij}$ is the magnetic vector angle. By loading the codes of all pixels into the geometry matrix **A**, the magnetic encoding matrix **M** can be obtained.

The calculation for magnetic vector angle $\boldsymbol{\theta}$ is based on two assumptions: (a) the rotation of a pixel's coordinate is equal to the rotation

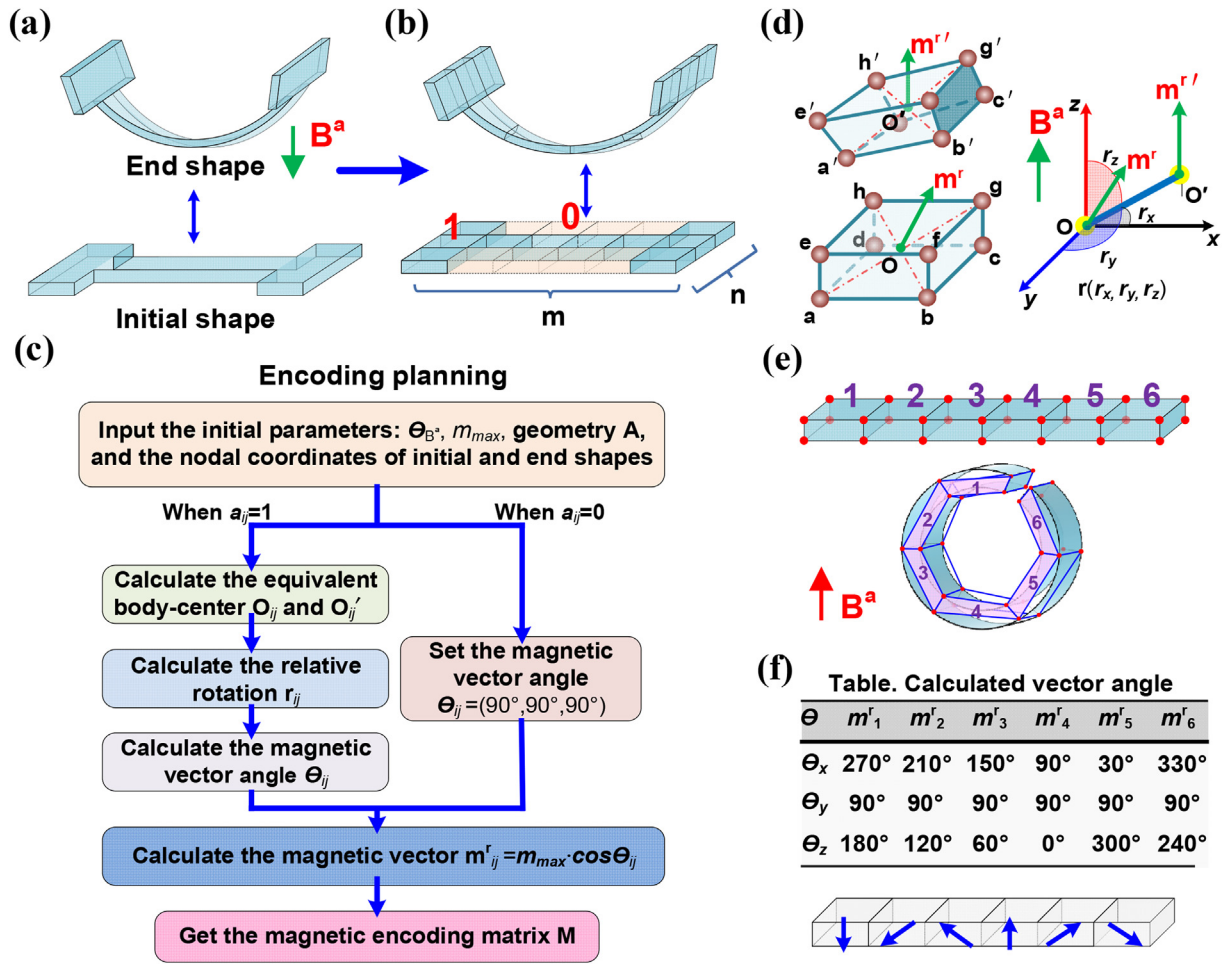

Figure 2. Magnetic encoding and deformation prediction: (a) Initial/end shape and pixelation, (b) Rotation of magnetization vector, (d) Encoding planning process, (e) Initial and end shape of the six-pixel inchworm robot, and (f) Calculated vector angle when $\boldsymbol{\theta}^a_B$= (90°,90°,0°).

of its magnetization vector $\mathbf{m}^{\mathbf{r}}$; (b) the magnetic vector of each pixel will be parallel to the direction of the applied magnetic field $\mathbf{B}^{a}$ when the robot is in the end shape. It should be noted that elastic strain and gravity are not considered here. Figure 2d shows how to solve the rotation angle of the magnetic vector by using the equivalent body-centered relative displacement. For the *ij*-th pixel, the rotation angle $\mathbf{r}_{ij}$ is calculated according to Eq. (3),

$$\mathbf{r}_{ij} = \frac{\mathbf{O}'_{ij} - \mathbf{O}_{ij}}{\left|\mathbf{O}'_{ij} - \mathbf{O}_{ij}\right|} = \theta'_{ij} - \theta_{ij}, \tag{3}$$

where $\mathbf{O}_{ij}$ and $\mathbf{O}'_{ij}$ are the *ij*-th pixel's body-center coordinates of the initial and end shapes, respectively; $\boldsymbol{\theta}_{ij}'$ is the pixel's magnetic vector angle of the end shape.

A six-pixel inchworm robot is presented to demonstrate the encoding planning method. As shown in Figure 2e, the end shape of the proposed robot has meshed into six subsections, where the nodal coordinates of each subsection (pixel) are obtained. Figure 2f gives the calculated magnetic vector angle using the encoding planning program.

4. Material & fabrication

4.1. Preparation of Liquid-metal/NdFeB composites

The Liquid-metal and ferromagnetic composites are prepared by homogenously mixing liquid-phase gallium, with a melting point of 29.6 °C, purity of 99.9%, and neodymium-iron-boron micro-particles. The average particle size of $Nd_{14}Fe_2B$ (Xinnuode Transmition Devices Technique *co. Ltd*, Guangzhou, China) is 6.0 μm^3. As exhibited in Figure 3a, the mixture of unmagnetized NdFeB powder and liquid gallium, with a volume ratio of 4:6, is heated to 50 °C and stirred by a mechanical agitator in the air for 10 min. In Figure 3b, the Liquid-metal/NdFeB composites were magnetized in a pulsed magnetic field with magnetic strength of 2 T. The plasticity and low melting point of these composites are the basis of implementing magnetic encoding.

4.2. Fabrication of magnetic pixel film

A biocompatible material—Silicone (Ecoflex00-30, Smooth-On, America) is utilized for coating the liquid-metal/NdFeB composites. A template-assisted method was employed to prepare the magnetic pixel films (MPFs). As shown in Figure 3c, the coating process is divided into three steps, i.e., preparing the bottom shell, filling the composites, and packaging the top shell. Two 3D-printed molds were employed to fabricate the shells of the film, where the fabrication art is given in supplementary Text 1 and Figure S1. At last, two sizes of the pixel, i.e., 1 × 1 and 2 × 2 mm^2, are designed. The thickness of the shell and liquid-metal/NdFeB composites are 100 μm and 600 μm, respectively. Therefore, the total thickness of the functional film is 800 μm.

The physical parameters of the magnetic pixel are given in Table 1. The resolution of these MPFs are 1 × 1 and 2 × 2 mm^2, respectively. The maximum magnetization of a pixel is 2.4 mT. For efficient magnetic programming, the required heating temperature shall not be lower than 35 °C, while the minimum programming magnetic-field is 100 mT.

Table 1. Physical parameter of the magnetic pixel.

Dimensions	Maximum remanent magnetization m_{max}	Programming temperature	Resolution	Required programming magnetic-field $B_{p,min}$
1 × 1 × 0.8 or 2 × 2 × 0.8 mm^3	2.4 mT	>35 °C	1 or 2 mm^2	>100 mT

When manufacturing a magnetic pixel robot, a robot with a simple structure can be obtained by cutting on the magnetic pixel film. Furthermore, novel molds also can be used to prepare robots with complex structures. The magnetic pixel can be made into rectangular, triangular, or other shapes, depending on the shape of robot.

4.3. Thermal-magnetic coupled programming

As introduced in Section 2.1, a permanent magnet was utilized to generate the 3D vector programming magnetic field. In addition, a UV laser was adopted for heating a single magnetic pixel. With this thermal-magnetic coupling programming procedure, we can program the designed codes (as shown in Section 3 and 3.2) on the MPR. The magnetic flux density and laser-assist heating effect on a single pixel are given in Figure 4.

The magnet is fixed at 12 mm below the operation platform (Supplementary Figure S3). Figure 4a shows the programmed spatial magnetic-field distribution that acts on the magnetic pixel. We utilize the magnetic dipole model to calculate this simulation results (see Supplementary Text 2 and Figure S2). Figure 4b exhibits the measured values of some special directions (the coordinate- and 45° alignment directions), where the purple data represents the magnetic vector's modulus. Results show that the magnetic vector generated by the magnet in any direction is not less than 110 mT, which meets the requirements of the magnetization process.

The simulation and test results of laser heating on the 2 × 2 mm^2 resolution magnetic pixel film are given in Figure 4c and 4d. The laser spot area, heating period, and ambient temperature is 1.2 mm^2, 30 s, and 26.5 °C, respectively. In Figure 4c, the central point temperature of the pixel is 42.5 °C, the area of high-temperature region doesn't exceed 2 mm^2 (the simulation details are given in Supplementary Text 3). In Figure 4d, the surface temperature of the pixel film is measured by a thermal imager (HIKMICRO, China, 1 mm^2 resolution), where the central point temperature of the pixel film is 41.5 °C and the high temperature area is concentrated within 2 mm^2. The neighboring pixels's temperature of is below 30 °C. By adjusting the light spot area and heating period, thermal-magnetic programming can be carried out for smaller pixels.

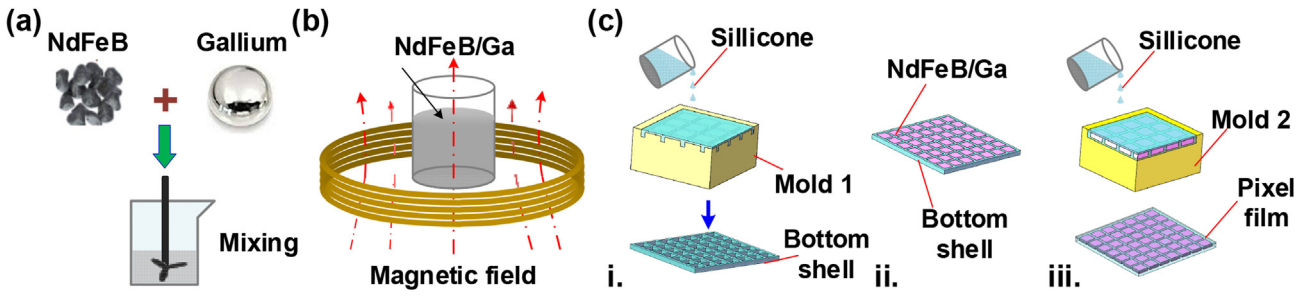

Figure 3. Fabrication process: (a) Mixing and (b) Magnetizing the NdFeB/Ga composites, (c) Preparing procedure.

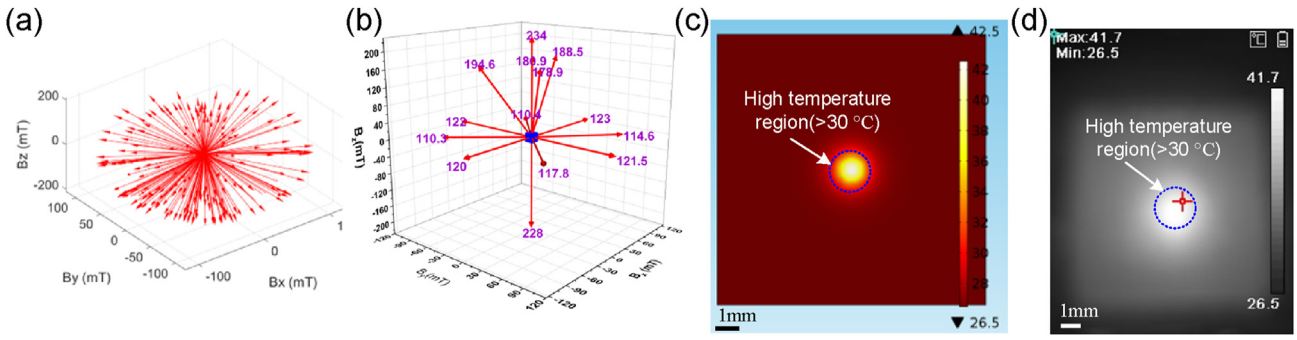

Figure 4. Thermal-magnetic coupled programming: (a) Simulation and (b) Measurement of the programming magnetic field, (c) Simulation and (d) Test of the laser-assist heating effect on a single magnetic pixel.

5. Experiments and discussion

5.1. Experimental results

In experiments, we tested the magnetic physical characteristics of the magnetic pixel film to prove its reprogrammability. Furthermore, some interesting patterning schemes were given to show the diversified programmable characteristics of magnetic pixel films. At last, we manufactured several magnetic soft robots. Consequently, we configured different encoding schemes on each MFSR, to generate multiple response actions.

The magnetic properties of the magnetic pixel film are tested by a physical property measurement system (PPMS). The applied magnetic-field is 10 kOe and the temperature changes from 273 to 373 K. The magnetization-temperature (M-T) and magnetization-magnetic field (M-H) curves are shown in Figure 5. In Figure 5a, a jump change of magnetization can be found at the temperature of 303 K, i.e., 30 °C. Consequently, the composites can continue to be magnetized when the temperature is higher than the melt point of gallium. In Figure 5b, the composites exhibit soft and hard magnetic properties respectively when at different temperature points, i.e., 293 and 313 K. The reason is that the gallium is in the solid-phase, and locks the NdFeB micro-particles at low-temperature. Accordingly, the material shows a macroscopical hard magnetic property. On the contrary, when the temperature rises and gallium is in the liquid phase, NdFeB particles can be aligned repeatedly under the action of the magnetic field. Therefore, this switchable "soft-/hard-magnetic", property of the Liquid-metal/NdFeB composites (Supplementary Text 4 and Figure S4) based on temperature regulation is the fundamental condition for achieving magnetic programming.

The basic magnetization performance of the magnetic pixel film is shown in Figure 6. Figure 6a and 6c exhibit the micro-graphs of the 2 × 2 and 1 × 1 mm^2 pixel film. We encoded the patterned form and Quick Response code (QR code) form of the letter "CAS" on the two films, respectively. The magnetic imaging photos of the two pixel films were observed by a high-sensitivity magnetic imaging card, as given in Figure 6b and 6d. Results show that the patterned magnetization profile scheme can be well implemented on the MPF. Two rectangular shape robots with 6-pixel and 22-pixel were directly cut off from the 2 × 2 mm^2 and 1 × 1 mm^2 pixel films, respectively. Circular deformation was then carried out for the rectangular shape robots. As given in Figure 6e and 6f, the higher the pixel resolution, the more circular the shape of the robot. Consequently, the robot can more smoothly simulate the preset end shape when using high-resolution magnetic pixels.

Figure 7a gives an improved multi-modal reptile robot composed of 15 magnetic pixels. Two different motion modes are implemented by encoding the robot. Figure 7b and 7c show that the robot acts like an inchworm, while Figure 7d and 7e show that the robot acts like a lizard. This case illustrates the possibility of applying different coding schemes to the same robot. Consequently, the multi-modal motion of the robot is easier to achieve. Furthermore, compared to traditional method [16], the multi-modal motion for MPSR is achieved by magnetic encoding, rather than relying on complex magnetic driving strategies. In this case, the driving strategy and motion performance are given in Supplementary Text 5, Figure S4 and movie 1.

Supplementary video related to this article can be found at https://doi.org/10.1016/j.heliyon.2022.e11415

Figure 8 shows the response of the cross-shape pixel robot when implemented with three different magnetic encodes. Figure 8a shows the photograph of the proposed robot, which composed of 9 pixels. As shown in Figure 8b and 8c, the robot performs as a fan with four blades. When using other magnetic encodes as in Figure 8d, the robot can stand up, as

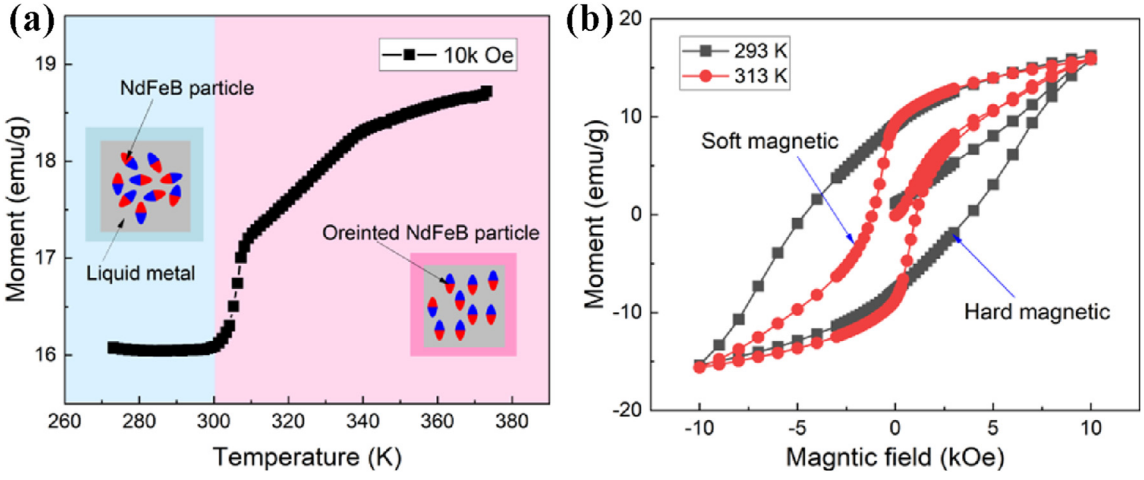

Figure 5. Magnetic properties of the magnetic pixel film: (a) M-T curve, (b) M-H curve.

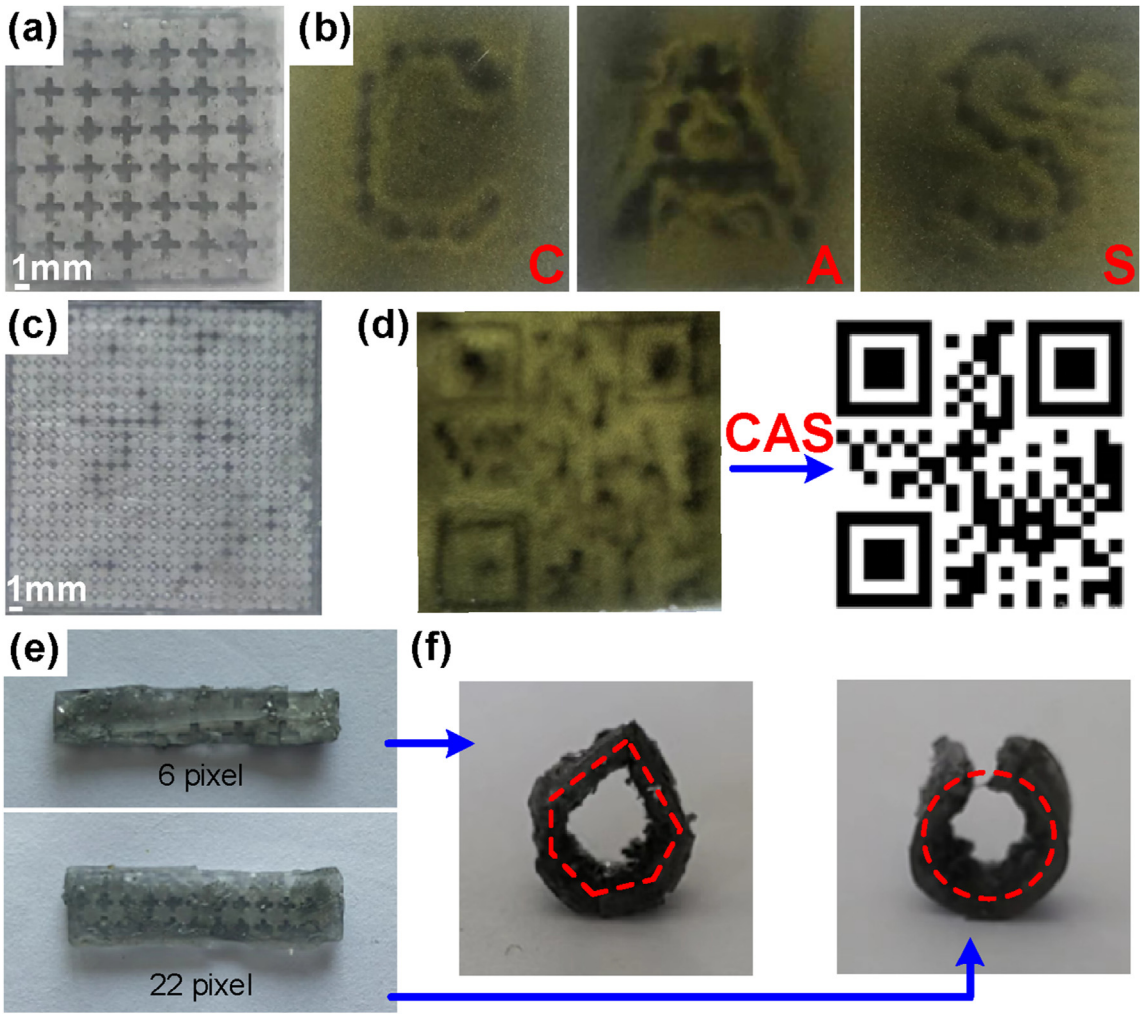

Figure 6. Patterning performance of the magnetic pixel film: (a) Photograph of 2 × 2 mm^2 magnetic pixel film, (b) Magnetic imaging of coding letters, (c) Photograph of 1 × 1 mm^2 magnetic pixel film, (d) Magnetic imaging of QR code, (e) 6-pixel and 22-pixel structures, (f) Circular shape deformation.

shown in Figure 8e. The robot also can function as a magnetic capsule to capture or transport a target, as shown in Figure 8f and 8g. These actions are all driven by a vertical magnetic field (see Supplementary Text 5, Figure S3 and movie 2).

Supplementary video related to this article can be found at https://doi.org/10.1016/j.heliyon.2022.e11415

Figure 9 exhibits a magnetic origami robot, consisting of eight triangular pixels. Four kinds of codes, i.e., Figure 9b, 9d, 9f, and 9h, are designed to generate different shapes of parallel folding, diagonal folding, pyramid deformation, and diagonal double folding, as shown in Figure 9c, 9e, 9g, and 9i, respectively. The driving strategy and motion performance of origami robot are given in Supplementary Text 5 and movie 3. According to the cases in Figures 6, 7, 8, and 9, a robot can be re-encoded to generate different response actions through repeatable magnetization techniques. This ability of reprogrammable shape enables the robot to perform various tasks.

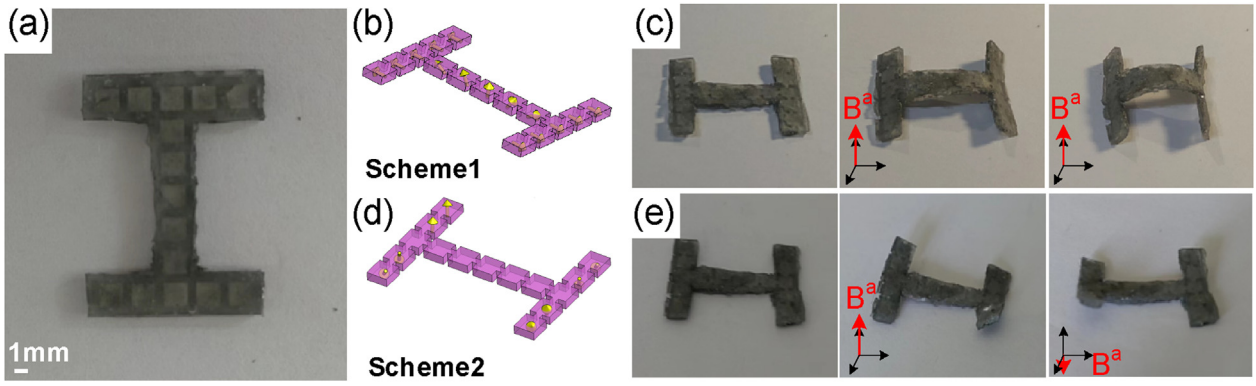

Figure 7. Encoding schemes and response actions of the improved multi-modal reptile robot: (a) Photograph of the proposed robot, (b) Encoding scheme 1 for inchworm-like motion and (c) Inchworm-like motion, (d) Encoding scheme 2 for crawling motion and (e) Crawling motion.

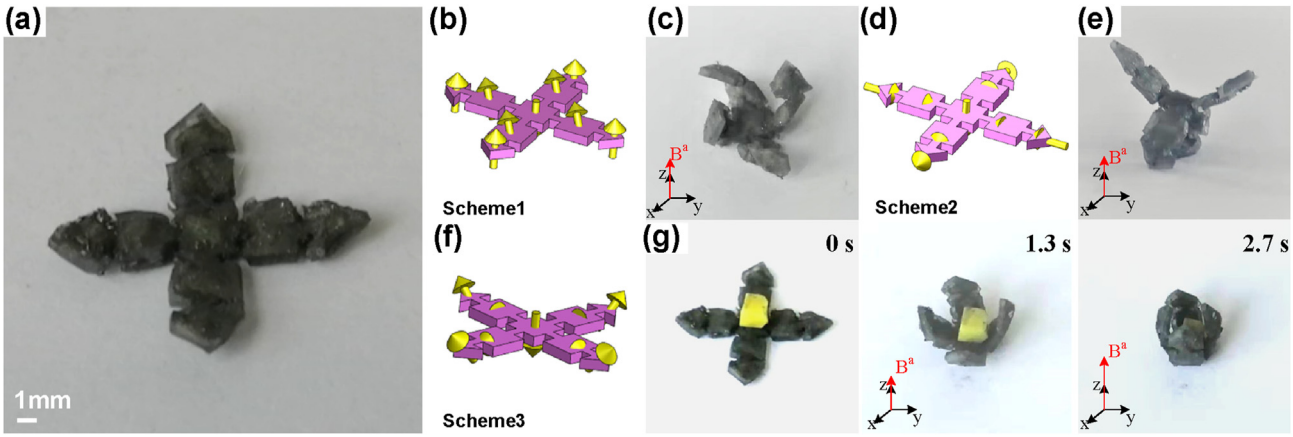

Figure 8. Encoding schemes and response actions of the cross-shape pixel robot: (a) Photograph of the cross-shape robot, (b) Encoding scheme 1 and (c) Fan action, (d) Encoding scheme 2 and (e) Standing action, (f) Encoding scheme 3 and (g) Grasping action.

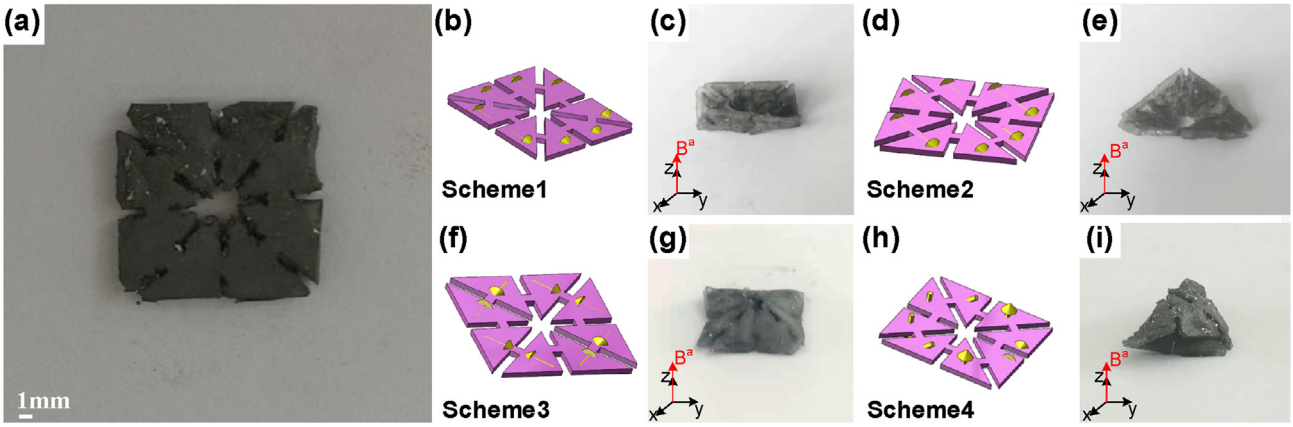

Figure 9. Encoding schemes and response actions of the magnetic origami robot: (a) Photograph of the proposed robot, (b) Encoding scheme 1 and (c) Parallel folding, (d) Encoding scheme 2 and (e) Diagonal folding, (f) Encode scheme 3 and (g) Pyramid deformation, (h) Encode scheme 4 and (i) Diagonal double folding.

Supplementary video related to this article can be found at https://doi.org/10.1016/j.heliyon.2022.e11415

As Figure 10 shows, a flexible z-axis positioning platform was built and tested. As shown in Figures 10a and 10b, the platform has a square flat and four support arms, which can move along the z-axis direction when applying a vertical magnetic field (see Supplementary Text 5 and movie 4). The encoding scheme and positioning curves are given in Figures 10c and 10d, respectively, where the maximum displacement is 3.1 mm under the magnetic field of 54.5 mT.

Supplementary video related to this article can be found at https://doi.org/10.1016/j.heliyon.2022.e11415

5.2. Discussion

Experimental results indicate that the MSPR can accomplish controllable deformation through magnetic encoding. Although we have only fabricated magnetic pixel with the highest resolution of 1 mm^2, the deformation and locomotion performance of MSPR is still very close to that of the continuous-structure MSR. In addition, the reprogrammability of MSPR allows us to reconfigure functions for different task requirements.

The reported magnetic programming techniques are analyzed and compared. As shown in Table 2, mostly magnetization profile methods

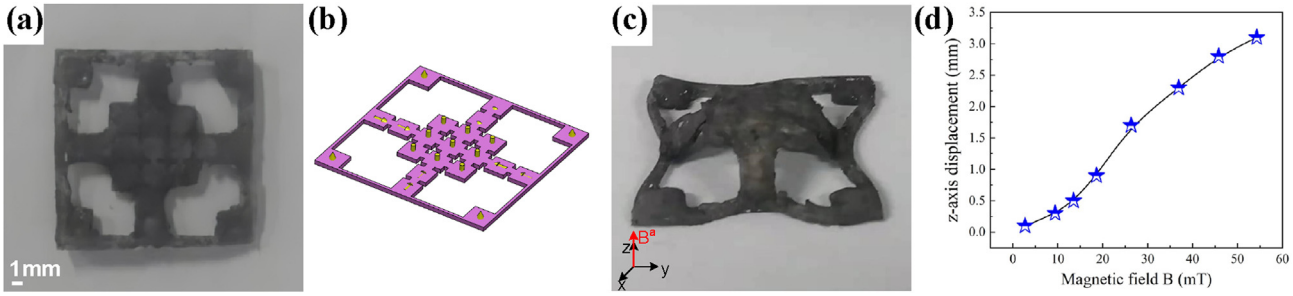

Figure 10. Performance of the magnetic flexible z-axis platform: (a) Photograph of the platform, (b) Encoding scheme, (c) Moving along z-axis direction when applying a magnetic field and (d) The z-axis displacement.

Table 2. Comparison of magnetic programming (encoding) techniques.

Refs.	Materials	Method description (magnetic field, program mode, program temperature, magnetization profile, and repeatability)
[16]	NdFeB/Ecoflex	Fixed direction field, whole programming, room temperature,experience-based magnetization profile design, unrepeatable
[18]	NdFeB/UV resin	3D vector field, laser-assisted local programming, room temperature experience-based magnetization profile design, unrepeatable
[12]	CrO_2/PDMS	3D vector field, laser-assisted local programming, >120 °C, experience-based magnetization profile design, repeatable
[20]	NdFeB/Ga/Silicone	3D vector field, heating-free local programming, room temperature, experience-based magnetization profile design, repeatable
[21]	NdFeB/Ecoflex	2D vector field, printed local programming, room temperature, experience-based magnetization profile design, unrepeatable
[19]	Nano Co/PMMA	2D vertical directional field, discrete encoding, room temperature, experience-based magnetization profile design, repeatable
[22]	NdFeB/PCL/Silicone	3D vector field, Laser-assisted local programming, >60 °C, experience-based magnetization profile design, repeatable
This study	NdFeB/Ga/Ecoflex	3D vector field, laser-assisted discrete encoding, >40 °C, calculation-based magnetization profile design, repeatable

are based on experience [12, 16, 18, 20, 21, 22], where the magnetization process is unrepeatable [16, 18, 21]. The programming temperature is another crucial technical issue. Compared with the existing repetitive 3D magnetic programming technique [12, 22]. The proposed technology has lower programming temperature. Consequently, less energy and less impact on the property of magnetic composites can be required.

In summary, the proposed technique has superiority since it decouples the MSR's magnetic programming and manufacturing process. Furthermore, this superiority yields calculation-based encoding planning and reprogrammable magnetization. Eventually, the deformation design of MSR is simplified.

6. Conclusion

This study presents a magnetic pixel soft robot with a programmable shape morphing function. Inheriting the achievements of our previous work [20], we employed liquid metal and NdFeB to construct the magnetic pixel. Using a standard encoding procedure and a mathematical model, we implemented the automatic planning for the magnetization profile of MSPR. A special 3D vector magnetization equipment was developed to program the MSPR. Finally, several cases exhibit the performance of MSPR. Results show that this technique has excellent application prospects in the automatic deformation planning and function design of MSR. The main contributions of this study are:

i. Designed a lattice-structure magnetic pixel robot based on Liquid-metal/NdFeB composites. The robot can fit the deformation of the continuum by using discrete regions, thereby reprograming its shape morphing.
ii. Proposed a 3D magnetic vector encoding technique and a standard procedure for code planning. This technique achieves automatic deformation design.

It should be pointed out that the technique still has limitations. Limited by the manufacturing technique, we can only produce pixels with the highest resolution of 1 mm^2. The template-aided manufacturing method is not suitable for mass production of MSPR. The 3D printing technique [14, 23] is expected to solve the problem of batch manufacturing. The computational encoding model does not consider the effects of gravity and strain. The constitutive law of hard-magnetic soft materials should be introduced to the model.

Eventually, the magnetic pixel robot provides a novel approach to the design of magnetic soft robots. In the future, artificial intelligence algorithms are expected to be employed in designing and manufacturing magnetic soft robots. Therefore, the next stage of this study is to reduce the size of magnetic pixels, thereby manufacturing milli- or micro-scale MPSR.

Declarations

Author contribution statement

Ran Zhao: Conceived and designed the experiments; Performed the experiments; Analyzed and interpreted the data; Wrote the paper.

Houde Dai: Conceived and designed the experiments; Wrote the paper.

Hanchen Yao, Guopeng Zhou: Performed the experiments.

Yafeng Shi: Contributed reagents, materials, analysis tools or data.

Funding statement

Ran Zhao was supported by Chinese Postdoctoral Science Foundation [2021M700780] and Special Fund Project for Basic Business of Zhongyuan University of Technology [K2022YY008].

Houde Dai was supported by the Central Guidance on Local Science and Technology Development Fund of Fujian Province [2021L3047] and [20d0581bfa].

Data availability statement

Data included in article/supp. material/referenced in article.

Declaration of interest's statement

The authors declare no conflict of interest.

Additional information

Supplementary content related to this article has been published online at https://doi.org/10.1016/j.heliyon.2022.e11415.

References

[1] L.X. Lyu, F. Li, K. Wu, P. Deng, S.H. Jeong, Z. Wu, H. Ding, Bio-inspired untethered fully soft robots in liquid actuated by induced energy gradients, Natl. Sci. Rev. 6 (5) (2019) 970–981.
[2] J.J. Wie, M.R. Shankar, T.J. White, Photomotility of polymers, Nat. Commun. 7 (2016), 13260.
[3] M. Wehner, R.L. Truby, D.J. Fitzgerald, B. Mosadegh, G.M. Whitesides, J.A. Lewis, R.J. Wood, An integrated design and fabrication strategy for entirely soft, autonomous robots, Nature 536 (2016) 451–455.
[4] J. Shintake, S. Rosset, B. Schubert, D. Floreano, H. Shea, Versatile soft grippers with intrinsic electroadhesion based on multifunctional polymer actuators, Adv. Mater. 28 (2015) 231–238.
[5] F.Y. Wu, S. Foong, Z. Sun, A hybrid field model for enhanced magnetic localization and position control, IEEE Trans. Mechatron. 20 (3) (2015) 1278–1287.
[6] D. Ye, J. Xue, S. Yuan, F. Zhang, S. Song, J. Wang, M.Q.-H. Meng, Design and control of a magnetically-actuated capsule robot with biopsy function, IEEE Trans. Biomed. Eng. 69 (9) (2022) 2905–2915.
[7] C. Hu, S. Pane, B.J. Nelson, Soft micro and nano robotics, Annu. Rev. Control, Robot. Autonom. Syst. 1 (1) (2018) 53–75.
[8] N. Ebrahimi, C. Bi, D.J. Cappelleri, G. Ciuti, A.T. Conn, D. Faivre, N. Habibi, A. Hoovsk, V. Iacovacci, I.S.M. Khalilet, Magnetic actuation methods in bio/soft robotics, Adv. Funct. Mater. 31 (11) (2020), 2005137.
[9] J. Zhang, E. Diller, Untethered miniature soft robots: modeling and design of a millimeter-scale swimming magnetic sheet, Soft Robot. (2017), 0126.

[10] H. Gu, Q. Boehler, H. Cui, E. Secchi, G. Savorana, D.C. Marco, S. Gervasoni, Q. Peyron, T.Y. Huang, S. Pane, A. Hirt, D. Ahmed, J.B. Nelson, Magnetic cilia carpets with programmable metachronal waves, Nat. Commun. 11 (2020) 2637.
[11] H. Huang, M.S. Sakar, A.J. Petruska1, S. Pane, B.J. Nelson, Soft micromachines with programmable motility and morphology, Nat. Commun. 7 (2016), 12263.
[12] Y. Alapan, A.C. Karacakol, S.N. Guzelhan, I. Isik, M. Sitti, Reprogrammable shape morphing of magnetic soft machines, Sci. Adv. 6 (2020), eabc6414.
[13] Y. Kim, G.A. Parada, S. Liu, X. Zhao, Ferromagnetic soft continuum robots, Sci. Robot. 4 (2019), eaax7329.
[14] F. Zhang, L. Wang, Z. Zheng, Y. Liu, J. Leng, Magnetic programming of 4D printed shape memory composite structures, Compos. Part A 125 (2019), 10557.
[15] Q. Ze, X. Kuang, S. Wu, Magnetic shape memory polymers with integrated multifunctional shape manipulation, Adv. Math. (2019), 1906657.
[16] W. Hu, G.Z. Lum, M. Mastrangeli, M. Sitti, Small-scale soft-bodied robot with multimodal locomotion, Nature 554 (2018) 81–85.
[17] L. Manamanchaiyaporn, T. Xu, X. Wu, Magnetic soft robot with the triangular head-tail morphology inspired by lateral undulation, IEEE Trans. Mechatron. 25 (6) (2020) 2688–2699.
[18] T. Xu, J. Zhang, M. Salehizadeh, O. Onaizah, E. Diller, Millimeter-scale flexible robots with programmable three-dimensional magnetization and motions, Sci. Robot. 4 (2019), eaav4494.
[19] J. Cui, T. Huang, h. Luo, Nanomagnetic encoding of shape-morphing micromachines, Nature 575 (2019) 7.
[20] R. Zhao, H. Dai, H. Yao, Liquid-metal magnetic soft robot with reprogrammable magnetization and stiffness, IEEE Rob. Autom. Lett. 7 (2) (2022) 4535–4541.
[21] Y. Kim, H. Yuk, R. Zhao, S.A. Chester, X. Zhao, Printing ferromagnetic domains for untethered fast-transforming soft materials, Nature 558 (2019) 274–279.
[22] H. Deng, K. Sattari, Y. Xie, Laser reprogramming magnetic anisotropy in soft composites for reconfigurable 3D shaping, Nat. Commun. 11 (2020) 6325.
[23] B. Sun, R. Jia, H. Yang, X. Chen, K. Tan, Q. Deng, J. Tang, Magnetic arthropod millirobots fabricated by 3D-printed hydrogels, Adv. Intell. Syst. (2021), 2100139.